



HAL
open science

Evolution of ac Conductivity in Nonequilibrium Warm Dense Gold

Z. Chen, B. Holst, S. Kirkwood, V. Sametoglu, M. Reid, Y. Tsui, V. Recoules,
A. Ng

► **To cite this version:**

Z. Chen, B. Holst, S. Kirkwood, V. Sametoglu, M. Reid, et al.. Evolution of ac Conductivity in Nonequilibrium Warm Dense Gold. *Physical Review Letters*, 2013, 110 (13), 10.1103/PhysRevLett.110.135001 . hal-02559135

HAL Id: hal-02559135

<https://hal.science/hal-02559135v1>

Submitted on 16 Mar 2022

HAL is a multi-disciplinary open access archive for the deposit and dissemination of scientific research documents, whether they are published or not. The documents may come from teaching and research institutions in France or abroad, or from public or private research centers.

L'archive ouverte pluridisciplinaire **HAL**, est destinée au dépôt et à la diffusion de documents scientifiques de niveau recherche, publiés ou non, émanant des établissements d'enseignement et de recherche français ou étrangers, des laboratoires publics ou privés.



Distributed under a Creative Commons Attribution 4.0 International License

Evolution of ac Conductivity in Nonequilibrium Warm Dense Gold

Z. Chen,¹ B. Holst,^{2,3} S. E. Kirkwood,⁴ V. Sametoglu,¹ M. Reid,⁵ Y. Y. Tsui,¹ V. Recoules,^{2,6} and A. Ng^{7,*}

¹Department of Electrical and Computer Engineering, University of Alberta, Edmonton, Alberta, Canada

²CEA, DAM, DIF, 91297 Arpajon, France

³LULI, École Polytechnique, CNRS, UPMC, route de Saclay, 91128 Palaiseau, France

⁴Department of Physics, University of Ottawa, Ottawa, Ontario, Canada

⁵Department of Physics, University of Northern British Columbia, Prince George, British Columbia, Canada

⁶LUTH UMR8102, Observatoire de Paris, CNRS, Université Paris Diderot, 92195 Meudon, France

⁷Department of Physics and Astronomy, University of British Columbia, Vancouver, British Columbia, Canada

(Received 4 August 2012; published 26 March 2013)

Using a chirped pulse probe technique, we have obtained single-shot measurements of temporal evolution of ac conductivity at 1.55 eV (800 nm) during electron energy relaxation in nonequilibrium warm dense gold with energy densities up to 4.1 MJ/kg (8×10^{10} J/m³). The results uncover important changes that have been masked in an earlier experiment. Equally significant, they provide valuable tests of an *ab initio* model for the calculation of electron heat capacity, electron-ion coupling, and ac conductivity in a single, first principles framework. While measurements of the real part of ac conductivity corroborate our theoretical temperature-dependent electron heat capacity, they point to an electron-ion coupling factor of $\sim 2.2 \times 10^{16}$ W/m³ K, significantly below that predicted by theory. In addition, measurements of the imaginary part of ac conductivity reveal the need to improve theoretical treatment of intraband contributions at very low photon energy.

DOI: [10.1103/PhysRevLett.110.135001](https://doi.org/10.1103/PhysRevLett.110.135001)

PACS numbers: 52.50.Jm, 52.27.Gr, 71.15.-m, 72.80.-r

Warm dense matter refers to states in which electron temperature is comparable to Fermi energy and ion-ion interaction potential exceeds ion kinetic energy. As a key transport coefficient, electrical conductivity of warm dense matter has long been of interest, driven by the breakdown of Spitzer theory [1] in that regime. An early remedy was provided by Lee and More [2] using the Boltzmann equation in relaxation time approximation with legislated cutoffs on impact parameters for Coulomb scattering. Their model was corroborated by reflectivity measurements obtained from shock compressed and released states of aluminum [3]. Shortly after, a more formal approach to calculate dc resistivity of Xe and Al plasmas was described by Perrot and Dharma-wardana, using the extended Ziman formula and density-functional theory [4]. A new measurement of reflectivity of femtosecond laser-heated Al also emerged and the results were used to determine dc resistivity [5]. This drew particular attention because of its substantial disagreement with calculations based on phase space particle-particle correlation function in kinetic theory [6]. The discrepancy was later resolved by comparing reflectivity measured by Milchberg *et al.* [5] and Fedosejevs *et al.* [7] directly with simulations that took into account hydrodynamic expansion and nonlocal interaction of incident laser field [8], where both experiments were found to be consistent with theory [2,4]. On the other hand, a new discrepancy appeared in the measurement of dc conductivity of copper and aluminum plasmas at $10^4 - 3 \times 10^4$ K and less than one-fifth solid density by DeSilva and Katsouras in 1998 [9]. Their data deviated

significantly from predictions of the Lee and More model. This was attributed by Desjarlais *et al.* [10] to metal-nonmetal transition in expanded copper, as demonstrated in their density-functional-theory calculations together with the Kubo-Greenwood formula. Further studies of electrical conductivity of expanded Cu and Al were reported respectively by Clérouin *et al.* [11] and Faussurier *et al.* [12]. Also in 1998, a new approach to measure ac conductivity of the uniform warm dense matter state based on isochoric laser heating of ultrathin metal foils was described by Forsman *et al.* using numerical simulations [13]. This was demonstrated by Widmann *et al.* in the measurement on gold [14]. The work prompted the calculation of ac conductivity under nonequilibrium conditions in the framework of density-functional theory and the Kubo-Greenwood formula by Mazevet *et al.* [15]. Their results showed good agreement with experiment if the observed state was superheated solid gold with hot electrons and cold ions. Such a state was confirmed in broadband dielectric function measurements by Ping *et al.* [16]. In spite of their success, the two experiments [14,16] left important open questions. The apparently constant ac conductivity throughout the superheated solid phase that lasted for ~ 20 ps for energy density of 0.5 MJ/kg to ~ 2 ps for energy density of 20 MJ/kg [17] seemed anomalous. Over such durations, ion temperature would increase and electron temperature decrease due to electron-ion coupling, leading to changes in ac conductivity. This led to the conjecture that such changes were masked by limited shot-to-shot reproducibility of data

collected from multiple shots. Resolution of the anomaly is critical. It is key to understanding the behavior of electron energy relaxation and two-temperature ac conductivity in nonequilibrium warm dense matter.

Here, we present measurements of temporal evolution of ac conductivity in nonequilibrium warm dense gold, using a single-shot pump-probe technique. The 400 nm-pump and 800 nm-probe pulses are derived from an 800 nm, 45 fs (FWHM) main laser. The pump pulse was focused to a $62 \mu\text{m}$ -diameter Gaussian spot (FWHM) at normal incidence on a freestanding gold foil (29.4–29.8 nm thick) with maximum intensity of $2 \times 10^{13} \text{ W/cm}^2$. Prepulse contrast in the 800 nm laser beam is 10^{-4} at 0.5 ps before pulse peak [18]. The corresponding contrast at 400 nm is expected to be $\sim 10^{-8}$. Absorbed laser energy is determined from simultaneous measurements of incident, reflected, and transmitted pump pulses with $5 \mu\text{m}$ spatial resolution. Laser absorption occurs by skin-depth deposition in a $\sim 16 \text{ nm}$ -thick layer beneath the surface of the gold foil [19], causing excitation of $5d$ electrons to states above the Fermi level. Thermalization time for these nonthermal electrons is $\sim 600 \text{ fs}$ [20,21]. This is much longer than the laser pulse duration. The absorbed laser energy is thus carried into the foil by ballistic transport of nonthermal electrons. Since the ballistic electron range in gold is $\sim 100 \text{ nm}$ [22,23], which far exceeds foil thickness, some nonthermal electrons may escape from the foil only to be returned by space charge fields leading to refluxing. The combined processes of ballistic electron transport and refluxing then produces uniform heating of the gold foil as observed for an absorbed laser flux up to $\sim 7 \times 10^{12} \text{ W/cm}^2$ or an excitation energy density $\Delta\epsilon$ of 10^{11} J/m^3 or 5.4 MJ/kg [24]. The 800 nm-probe pulse is P polarized to enhance sensitivity to ac conductivity of the heated state. It is chirped to a duration of 6.5 ps (FWHM) to provide a temporal record of reflected and transmitted signals in a single shot. Temporal resolution of the chirped pulse probe is estimated to be 540 fs. It is collimated to illuminate the front surface of target foil in a 1 mm-diameter spot at 45-degree incidence. The reflected and transmitted probe lights are each imaged onto a spectrometer with an entrance slit viewing a $20 \mu\text{m} \times 500 \mu\text{m}$ region, centered with the pump focal spot on the corresponding foil surface. Absolute values of reflectivity and transmissivity are obtained using *in situ* comparisons of signals from heated and unheated regions.

Figure 1 shows examples of temporal lineout of reflected and transmitted probe intensity obtained from the corresponding spectra. The high-frequency aperiodic oscillations are results of interference caused by pump-induced nonlinear optical Kerr effect as determined earlier [24]. To uncover the underlying intensity signals, we consider three temporal segments. The segment prior to laser heating and the segment during laser heating are approximated by linear functions. The postheating segment is extracted

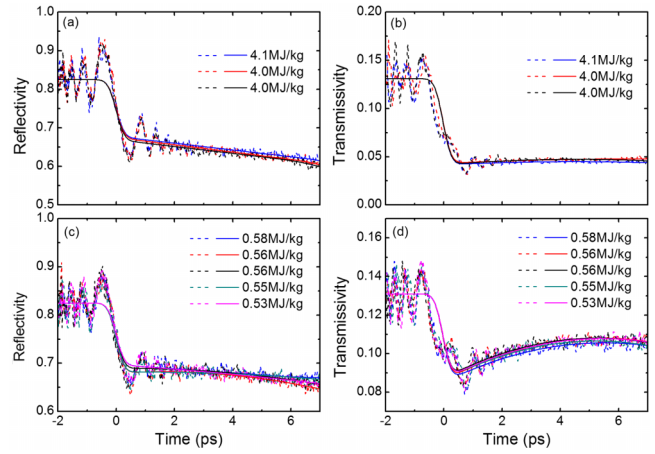


FIG. 1 (color online). Temporal changes in probe reflectivity and transmissivity for excitation energy densities of (a), (b) 4.0–4.1 MJ/kg, and (c), (d) 0.53–0.58 MJ/kg. Dotted lines are lineouts taken from measured spectra, and solid lines are the corresponding underlying intensity signals.

using a two-piece spline fit of a linear function that connects smoothly to a quadratic function. The combined signal, convoluted with a Gaussian instrumental function of 540 fs FWHM, is displayed by the solid lines in Fig. 1. These underlying intensity signals are then used to derive ac conductivity from solutions of the Helmholtz equations for electromagnetic wave propagation in a uniform dielectric slab [25]. Earlier studies have shown the persistence of a superheated solid up to $6 \pm 0.7 \text{ ps}$ after laser excitation at $\Delta\epsilon$ of 4.3 MJ/kg [16,17]. Accordingly, we have limited our measurements to pump-probe delays of $\leq 7 \text{ ps}$. It is clearly evident in Fig. 2 that ac conductivity does not remain constant during electron relaxation. In fact, $\sigma_r(t)$ appears to suggest competing effects are at play that lead to fall and rise in conductivity as electron temperature decreases and ion temperature increases.

In addition to eliminating the earlier anomaly of constant ac conductivity during electron energy relaxation,

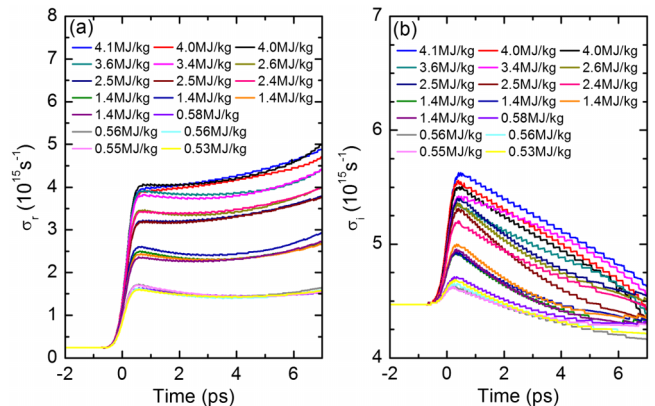


FIG. 2 (color online). (a) Real and (b) imaginary parts of ac conductivity as a function of pump-probe delays.

these new observations present a unique opportunity to test theoretical models of nonequilibrium warm dense matter, in particular quantum molecular dynamic simulations that allow calculations of physical properties in a single, first principles framework. In our present model, the electron system is described using the *ab initio* plane wave density functional theory (DFT) code ABINIT [26] in its parallel implementation [27]. For gold, DFT is applied together with local density approximation that yields a lattice constant in better agreement with known data than the generalized gradient approximation [28,29]. Simulations are performed with a cutoff energy of 16Ha, using a projected augmented wave (PAW) pseudopotential [30] with 11 valence electrons, which has been benchmarked extensively against measured physical properties [31]. In parallel, the ion system is described by molecular dynamic simulations performed with 108 ions in a cubic box. At each ionic time step, the electronic structure is calculated within DFT. Electron temperature T_e , which is controlled by the width of the Fermi-Dirac distribution, can be different from ion temperature T_i . Using this model, the real part of ac conductivity is calculated from the Kubo-Greenwood formula [32]. Integration over the Brillouin zone is done using $4 \times 4 \times 4$ Monkhorst-Pack k -point sampling [33]. The Kramers-Kronig relation is then applied to obtain the imaginary part of ac conductivity. Careful attention is paid to the Kramers-Kronig relation in terms of included empty valence bands. Extensive test calculations are made with an increased number of valence bands. To ensure convergence in the imaginary part of the ac conductivity below 5 eV, the band number is chosen to be ≥ 1024 . General applicability of the Kramers-Kronig relation to solid gold has been shown by applying it to the experimental data of [19]. Taking into account the expansion for low frequencies supplied therein, the calculated data exactly reproduce the measured imaginary part. The *ab initio* model further allows us to derive the electron heat capacity C_e as well as the electron-ion coupling factor g_{ei} that are needed in the application of a two-temperature model [34] to describe electron-ion equilibration. Specifically, C_e is given by the temperature derivative of electron internal energy at constant volume that takes into account excitations and changes in both position and shape of electron density of states at high T_e . Our calculation of g_{ei} is similar to that of Lin *et al.* in treating the electron-ion heat transfer rate with electron-phonon scattering in terms of electron and phonon occupation numbers [35], except for our use of a temperature-dependent electron density of states. Calculations were made at different T_e with a single atom in a primitive fcc cell using a $32 \times 32 \times 32$ k -point sampling grid. Figure 3 shows a comparison of C_e and g_{ei} , derived from our model, to those reported by Lin *et al.* for $T_i = 0$ K.

As the first test, we calculate ac conductivity of an initial heated state in which electrons are heated to a temperature

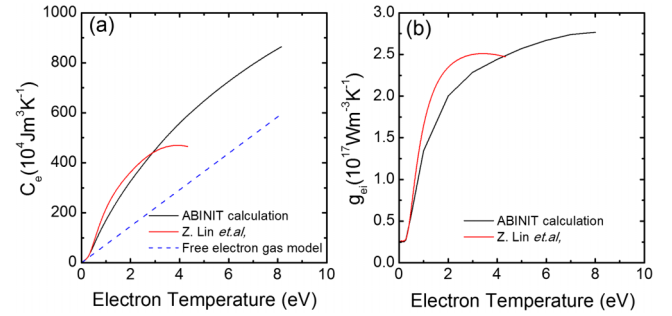


FIG. 3 (color online). Comparison of our calculated $C_e(T_e)$ and $g_{ei}(T_e)$ to those of Lin *et al.* [35].

T_e while the ions remain at T_i of 300 K. In accordance with the observed electron-electron thermalization time [20,21], such a state is taken to occur at 600 fs after the peak of pump laser pulse. We also assume that all absorbed laser energy resides in the electrons. This overestimates T_e and underestimates T_i , since energy transfer from electrons to ions would have started during the pump laser pulse. However, the discrepancy is expected to be small. Figure 4 shows a comparison of calculated ac conductivity of this initial heated state with corresponding measured values. Evidently, the measured values of σ_r agree much better with calculations using C_e derived from *ab initio* electron internal energy [Fig. 4(a)]. This becomes the first benchmark for our calculations of C_e and ac conductivity within a single, first principles framework. It is also a noteworthy corroboration of the calculated electronic structure in our model from which both C_e and ac conductivity are derived. On the other hand, substantial discrepancy between experiment and theory is seen in σ_i , although in the region above ~ 1 MJ/kg, the measured rate of change in σ_i with energy density appears to be consistent with calculations.

For a further test of our model, we turn to the subsequent evolution in ac conductivity, where energy exchange between electrons and ions can be described using a two-temperature-model [34,36] together with our calculated $C_e(T_e)$ and $g_{ei}(T_e)$. Here, ion heat capacity is taken to be

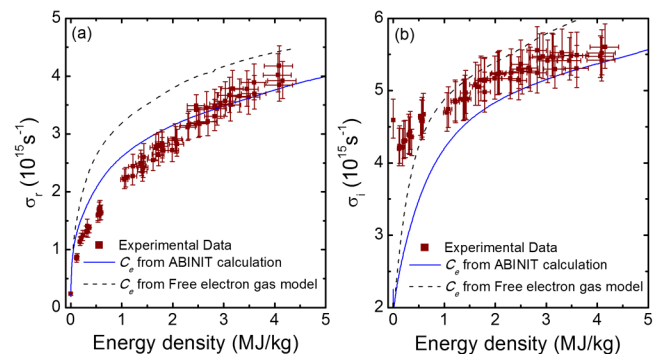


FIG. 4 (color online). (a) Real and (b) imaginary parts of initial ac conductivity as a function of excitation energy density.

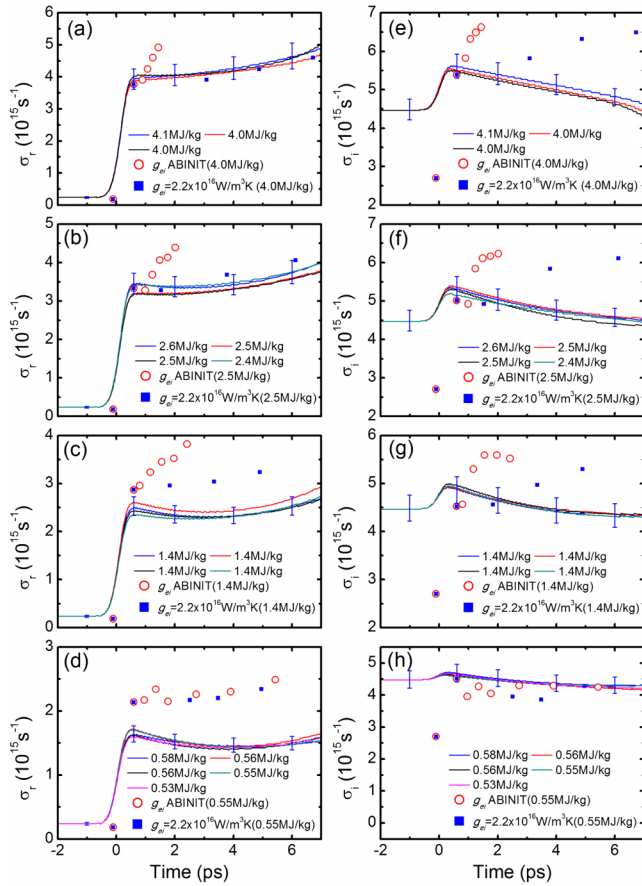


FIG. 5 (color online). Comparison of measured $\sigma_r(t)$ and $\sigma_i(t)$ to theoretical calculations for excitation energy densities of (a), (e) 4.0–4.1 MJ/kg, (b), (f) 2.4–2.7 MJ/kg, (c), (g) 1.4 MJ/kg, and (d), (h) 0.53–0.58 MJ/kg.

that of the lattice at a constant value of $2.5 \times 10^6 \text{ J/m}^3 \text{ K}$ [37], which does not change significantly at high T_e . This is consistent with our linear response calculations [38] using a fcc grid and $16 \times 16 \times 16$ k -point sampling on an $8 \times 8 \times 8$ q -point grid. For $\Delta\varepsilon > 1 \text{ MJ/kg}$ [Figs. 5(a)–5(c)], $\sigma_r(t)$ calculated from temperature-dependent g_{ei} predicts rapid increase with pump-probe delay. This differs significantly from observation that reveals initial decrease in $\sigma_r(t)$ followed by delayed onset of increase. To understand this discrepancy, we first note that as energy is transferred from electrons to ions, σ_r will decrease as T_e declines but increase as T_i rises. Evolution in σ_r is dictated by relative dominance of these two processes, which is in turn governed by g_{ei} . Interestingly, agreement between theory and experiment is greatly improved if $\sigma_r(t)$ is calculated using $g_{ei} = 2.2 \times 10^{16} \text{ W/m}^3 \text{ K}$ found in gold with $\Delta\varepsilon < 0.08 \text{ MJ/kg}$ [22]. This value is substantially lower than that derived from our calculation. For $\Delta\varepsilon < 1 \text{ MJ/kg}$, the choice of g_{ei} in the calculation of $\sigma_r(t)$ becomes much less critical. As is evident from the comparison at 0.53–0.58 MJ/kg [Fig. 5(d)], both calculations show a similar rate of change as observed in $\sigma_r(t)$ up to 7 ps after

the peak of pump laser pulse. This apparent lack of sensitivity to temperature effect on g_{ei} can be attributed to the low initial T_e of the heated foil and correspondingly small increase in the calculated temperature-dependent g_{ei} (Fig. 2). On the other hand, no satisfactory agreement can be found between theory and experiment for $\sigma_i(t)$ [Figs. 5(e)–5(g)] at any excitation energy density.

The observation of substantially lower than predicted g_{ei} for hot electrons and cold ions in laser-heated gold at $\Delta\varepsilon$ exceeding 1 MJ/kg is significant. This appears to mirror the earlier observation of a substantially lower than predicted g_{ei} in shock compressed silicon with hot ions and cold electrons [39]. The silicon study prompted development of the quantum mechanical, coupled mode approach [40] in which normal modes of electron oscillations exchange energy with an ion-acoustic mode (similar to ion-acoustic wave in plasmas) to take into account coupling of the electron cloud to the ions. Treating energy relaxation of hot electrons in Al with $T_i = 943 \text{ K}$, the coupled mode calculation revealed an electron-ion coupling factor that was more than an order of magnitude lower than those calculated from either the quantum mechanical Fermi golden rule approach in which normal modes of electron oscillations exchange energy with normal modes of ion oscillations (phonons) or the classical Spitzer model whereby energy exchange is derived from electron-ion scattering. Recently, Vorberger and Gericke [41] have also reported coupled mode calculations for Al at $T_i = 1000 \text{ K}$ showing values of g_{ei} an order of magnitude lower than those at $T_i = 300 \text{ K}$, comparable to those obtained by Dharma-wardana and Perrot at $T_i = 943 \text{ K}$ [40]. Accordingly, we attribute the disagreement between our observed and predicted values of g_{ei} to the absence of contributions due to finite T_i that is neglected in our model.

As discussed above, our model together with the Kubo-Greenwood formula provides reasonable calculations of σ_r in nonequilibrium warm dense gold. However, significant discrepancy is found in σ_i derived from the Kramers-Kronig relation. This discrepancy is traced to missing contributions to σ_r at energies below the energy difference ($\sim 0.1 \text{ eV}$) of the Kohn-Sham eigenstates in our application of the Kubo-Greenwood formula. Although only a small energy range is affected, this modifies the principal value integration within the Kramers-Kronig relation significantly. A recent study on sodium [42] implies that a solution for this problem is probably a higher number of simulated atoms which reduces the energy difference between eigenstates and improves the calculated dc conductivity. However, simulations with atom numbers of the order of 1000, which are necessary according to Ref. [42], on a grid of elevated electron temperature are beyond the scope of this study.

In conclusion, using a chirped pulse probe technique we have obtained single-shot measurements of temporal evolution of ac conductivity during electron energy

relaxation in nonequilibrium warm dense gold with $\Delta\epsilon$ up to 4.1 MJ/kg (8×10^{10} J/m³). The results have uncovered important changes that were masked in an earlier experiment. Equally important, they provide valuable tests of an *ab initio* model for the calculation of C_e , g_{ei} , and ac conductivity in a single, first principles framework. While the measured real part of ac conductivity corroborates our theoretical C_e , it points to a g_{ei} of $\sim 2.2 \times 10^{16}$ W/m³ · K that is significantly below our prediction. In addition, measurements of σ_i reveal the need to improve the theoretical treatment of intraband contributions at photon energy below 0.1 eV in the application of Kramers-Kronig relation.

We thank P. Renaudin, A. Sollier, and S. Mazevet for helpful discussions and the Advanced Laser Light Source in Canada for technical support and use of the facility. We acknowledge research support from the Natural Sciences and Engineering Research Council of Canada, Canadian Institute for Photonic Innovations, French Agence Nationale de la Recherche, Project OEDYP, Grant No. ANR-09-BLAN-0206. Part of the numerical calculations has been performed using resources from GENCI under Grant No. 6454.

*Corresponding author.

nga@physics.ubc.ca

- [1] L. Spitzer and R. Härm, *Phys. Rev.* **89**, 977 (1953).
- [2] L. More and R. M. More, *Phys. Fluids* **27**, 1273 (1984).
- [3] A. Ng, D. Parfeniuk, P. Celliers, L. DaSilva, R. M. More, and Y. T. Lee, *Phys. Rev. Lett.* **57**, 1595 (1986).
- [4] F. Perrot and M. W. C. Dharma-wardana, *Phys. Rev. A* **36**, 238 (1987).
- [5] H. M. Milchberg, R. R. Freeman, S. C. Davey, and R. M. More, *Phys. Rev. Lett.* **61**, 2364 (1988).
- [6] R. Cauble, F. J. Rogers, and W. Rozmus, in *Proc. SPIE Int. Soc. Opt. Eng.* **1229**, 211 (1990).
- [7] R. Fedosejevs, R. Ottmann, R. Sigel, G. Kühnle, S. Szatmari, and F. P. Schäfer, *Phys. Rev. Lett.* **64**, 1250 (1990).
- [8] A. Ng, P. Celliers, A. Forsman, R. M. More, Y. T. Lee, F. Perrot, M. W. C. Dharma-wardana, and G. A. Rinker, *Phys. Rev. Lett.* **72**, 3351 (1994).
- [9] A. W. DeSilva, and J. D. Katsourous, *Phys. Rev. E* **57**, 5945 (1998).
- [10] M. P. Desjarlais, J. D. Kress, and L. A. Collins, *Phys. Rev. E* **66**, 025401(R) (2002).
- [11] J. Clérouin, P. Renaudin, Y. Laudernet, P. Noiret, and M. P. Desjarlais, *Phys. Rev. B* **71**, 064203 (2005).
- [12] G. Faussurier, C. Blancard, P. Renaudin, and P. L. Silvestrelli, *J. Quant. Spectrosc. Radiat. Transfer* **99**, 153 (2006).
- [13] A. Forsman, A. Ng, G. Chiu, and R. M. More, *Phys. Rev. E* **58**, R1248 (1998).
- [14] K. Widmann, T. Ao, M. E. Foord, D. F. Price, A. D. Ellis, P. T. Springer, and A. Ng, *Phys. Rev. Lett.* **92**, 125002 (2004).
- [15] S. Mazevet, J. Clérouin, V. Recoules, P. M. Anglade, and G. Zerah, *Phys. Rev. Lett.* **95**, 085002 (2005).
- [16] Y. Ping, D. Hanson, I. Koslow, T. Ogitsu, D. Prendergast, E. Schwegler, G. Collins, and A. Ng, *Phys. Rev. Lett.* **96**, 255003 (2006).
- [17] T. Ao, Y. Ping, K. Widmann, D. F. Price, E. Lee, H. Tam, P. T. Springer, and A. Ng, *Phys. Rev. Lett.* **96**, 055001 (2006).
- [18] C. A. Popovici, R. A. Ganeev, F. Vidal, and T. Ozaki, *Advanced Laser Light Source Annual Report 2007–2008*, 2008, p. 48, http://lmn.emt.inrs.ca/EN/ALLS_Pub.htm.
- [19] P. B. Johnson and R. W. Christy, *Phys. Rev. B* **6**, 4370 (1972).
- [20] W. S. Fann, R. Storz, H. W. K. Tom, and J. Bokor, *Phys. Rev. Lett.* **68**, 2834 (1992); W. S. Fann, R. Storz, H. W. K. Tom, and J. Bokor, *Phys. Rev. B* **46**, 13592 (1992).
- [21] C. K. Sun, F. Vallee, L. Acioli, E. P. Ippen, and J. G. Fujimoto, *Phys. Rev. B* **48**, 12365 (1993).
- [22] J. Hohlfeld, S.-S. Wellershoff, J. Güdde, U. Conrad, V. Jähnke, and E. Matthias, *Chem. Phys.* **251**, 237 (2000).
- [23] J. Hohlfeld, J. G. Müller, S.-S. Wellershoff, and E. Matthias, *Appl. Phys. B* **64**, 387 (1997).
- [24] Z. Chen, V. Sametoglu, Y. Y. Tsui, T. Ao, and A. Ng, *Phys. Rev. Lett.* **108**, 165001 (2012).
- [25] T. Ao, Ph.D. thesis, University of British Columbia, 2004.
- [26] X. Gonze *et al.*, *Comput. Phys. Commun.* **180**, 2582 (2009).
- [27] F. Bottin, S. Leroux, A. Knyazev, and G. Zerah, *Comput. Mater. Sci.* **42**, 329 (2008).
- [28] A. D. Becke, *J. Chem. Phys.* **88**, 1053 (1988).
- [29] J. P. Perdew and Y. Wang, *Phys. Rev. B* **45**, 13244 (1992).
- [30] M. Torrent, F. Jollet, F. Bottin, G. Zerah, and X. Gonze, *Comput. Mater. Sci.* **42**, 337 (2008).
- [31] A. Dewaele, M. Torrent, P. Loubeyre, and M. Mezouar, *Phys. Rev. B* **78**, 104102 (2008).
- [32] S. Mazevet, M. Torrent, V. Recoules, and F. Jollet, *High Energy Density Phys.* **6**, 84 (2010).
- [33] H. J. Monkhorst and J. D. Pack, *Phys. Rev. B* **13**, 5188 (1976).
- [34] S. I. Anisimov, B. L. Kapeliovich, and T. L. Perel'man, *Sov. Phys. JETP* **39**, 375 (1974) [http://www.jetp.ac.ru/cgi-bin/dn/e_039_02_0375.pdf].
- [35] Z. Lin, L. V. Zhigilei, and V. Celli, *Phys. Rev. B* **77**, 075133 (2008).
- [36] The application of two-temperature model in the treatment of fs-laser-heated solids has been described broadly in the literature since the work of H. E. Elsayed-Ali, T. B. Norris, M. A. Pessot, and G. A. Mourou, *Phys. Rev. Lett.* **58**, 1212 (1987); R. W. Schoenlein, W. Z. Lin, J. G. Fujimoto, and G. L. Eesley, *Phys. Rev. Lett.* **58**, 1680 (1987); S. D. Brorson, J. G. Fujimoto, and E. P. Ippen, *Phys. Rev. Lett.* **59**, 1962 (1987).
- [37] A. M. James and M. P. Lord, *MacMillan's Chemical and Physical Data* (MacMillan Press, London, 1972).
- [38] X. Gonze and C. Lee, *Phys. Rev. B* **55**, 10355 (1997).
- [39] P. Celliers, A. Ng, G. Xu, and A. Forsman, *Phys. Rev. Lett.* **68**, 2305 (1992).
- [40] M. W. C. Dharma-wardana and F. Perrot, *Phys. Rev. E* **58**, 3705 (1998); *Phys. Rev. E* **63**, 069901(E) (2001).
- [41] J. Vorberger and D. O. Gericke, *AIP Conf. Proc.* **1464**, 572 (2012).
- [42] M. Pozzo, M. P. Desjarlais, and D. Alfè, *Phys. Rev. B* **84**, 054203 (2011).